Electronic Supplementary Information (ESI)

Microbial electrosynthesis with *Clostridium ljungdahlii* benefits from hydrogen electron mediation and permits a greater variety of products

Santiago T. Boto[a, b], Bettina Bardl[a], Falk Harnisch[c], Miriam A. Rosenbaum[a, b*]

a. Leibniz Institute for Natural Product Research and Infection Biology - Hans Knöll Institute (HKI), Beutenbergstraße 13, 07745 Jena, Germany

b. Faculty of Biological Sciences, Friedrich Schiller University, Bachstraße 18k, 07743 Jena, Germany

c. UFZ - Helmholtz-Centre for Environmental Research GmbH, Department of Environmental Microbiology, Permoserstraße, 15, 04318 Leipzig, Germany

*Corresponding author: Miriam A. Rosenbaum, miriam.rosenbaum@leibniz-hki.de

Number of Pages: 18
Number of Figures: 14
Number of Tables: 1

Contents:

1. Additional materials and methods

1.1 Plasmid construction and genetic manipulation

Phusion® high-fidelity DNA polymerase, plasmid DNA extraction, and DNA gel extraction kits were purchased from New England BioLabs (Ipswich, USA) and used following the manufacturer's instructions. FastDigest restriction enzymes, FastAP phosphatase and T4 DNA ligase were purchased from Thermo Fisher Scientific (Waltham, USA) and used following the manufacturer's instructions.

The plasmid pFAST(thl) for the expression of the FAST anaerobic fluorescent protein[1] was built starting from the plasmid pMTL83151[2]. The FAST gene was commercially synthetized (Eurofins Genomics, Ebersberg, Germany), digested and ligated into pMTL83151 using AatII and NotI. The constitutive *thl* promoter was amplified from the plasmid pMTL82152[2], digested and ligated upstream of the FAST gene using BglII and AatII. The final plasmid was methylated with *E. coli* pANA1 and introduced into *C. ljungdahlii* through a modified electroporation protocol[3]. Briefly, 10 mL of *C. ljungdahlii* culture within an OD600 range of 0.3-0.6 were collected by centrifugation at 1500 rcf for 2 min. The cell pellets were washed twice with 10 % glycerol and resuspended in 200 µL of 10 % glycerol. Electroporation was performed using 2 µg of plasmid DNA in 2 mm electroporation cuvettes using the following parameters: 2500 V, 10 µF, 600 Ω (Gene Pulser Xcell Microbial System; Bio-Rad Laboratories, Hercules, USA). The transformants were recovered in RCM medium without antibiotics for 20-24 h, and then cultured in RCM supplemented with thiamphenicol (5 µg/mL). The correct transformants of the constructed strain *C. ljungdahlii* pFAST(thl) were confirmed by plasmid rescue and Sanger sequencing.

Table S1. Synthesized gene and primers used for this work.

Name	Resource	Sequence (5'-3')
γFAST optimized	Synthesized gene between AatII and NotI sites in the plasmid pEX-A128	ATGGAACATGTAGCATTTGGATCTGAA GATATAGAAAATACTTTAGCAAAAATG GATGATGGACAATTAGATGGATTAGCA TTTGGAGCAATACAATTAGATGGAGAT GGAAATATATTACAATATAATGCAGCA GAAGGAGATATAACTGGAAGAGATCCT AAACAAGTAATAGGAAAAAATTTTTTT AAAGATGTAGCACCTGGAACTGATTCT CCTGAATTTTATGGAAAATTTAAAGAA GGAGTAGCATCTGGAAATTTAAATACT ATGTTTGAATGGATGATACCTACTTCT AGAGGACCTACTAAAGTAAAAGTACAT ATGAAAAAAGCATTATCTGGAGATTCT TATTGGGTATTTGTAAAAAGAGTATGA
thl_fwd_BglII	Forward primer for *thl* promoter amplification	CCCCCCAGATCTTTTTTAACAAAATAT ATTGATAAAAATAATAATAG
thl_rev_AatII	Reverse primer for *thl* promoter amplification	CCCCCCGACGTCAACTAACCTCCTAAA TTTTG

2. Additional figures and discussions

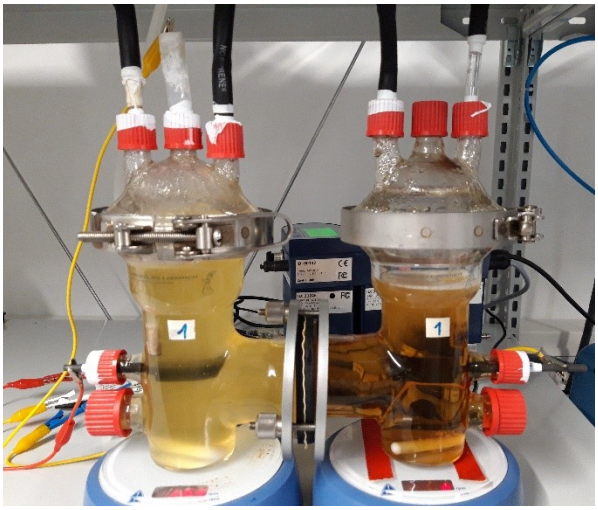

Figure S1. Picture of one glass H-type reactor used in the experiments. Growth can be observed as turbidity in the cathodic chamber (left).

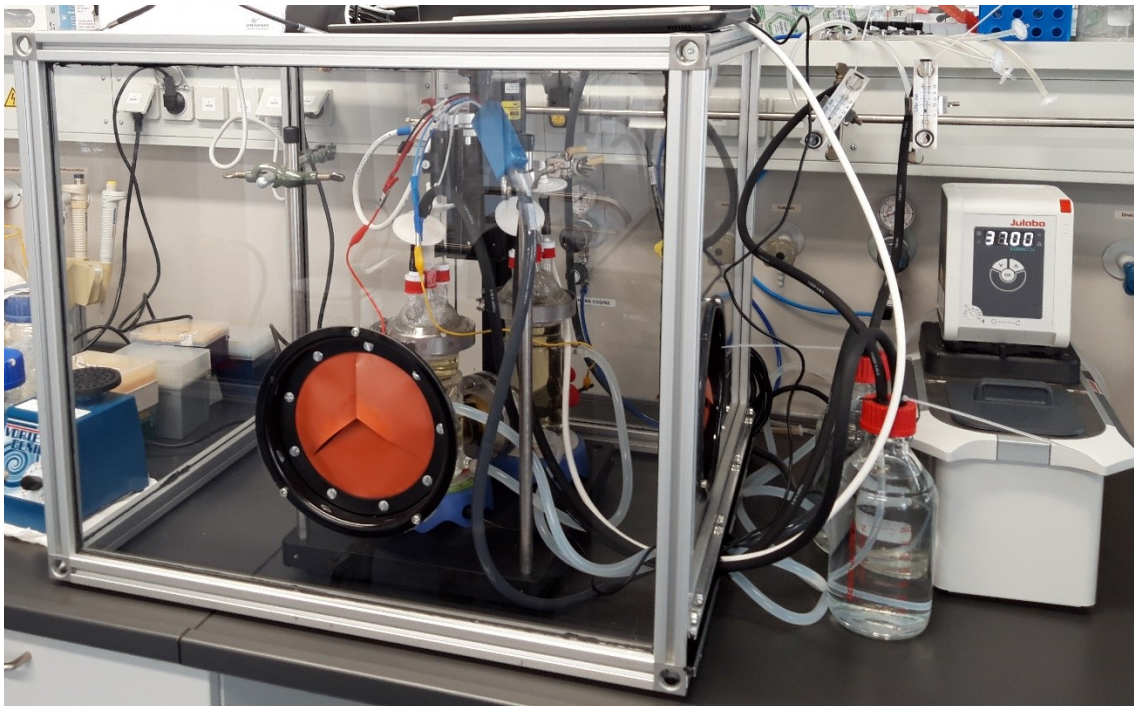

Figure S2. Picture of the customized anaerobic chamber for the experiments with the microsensors that allowed to open the lids of the H-type reactor (mounted inside) in order to perform the measurements.

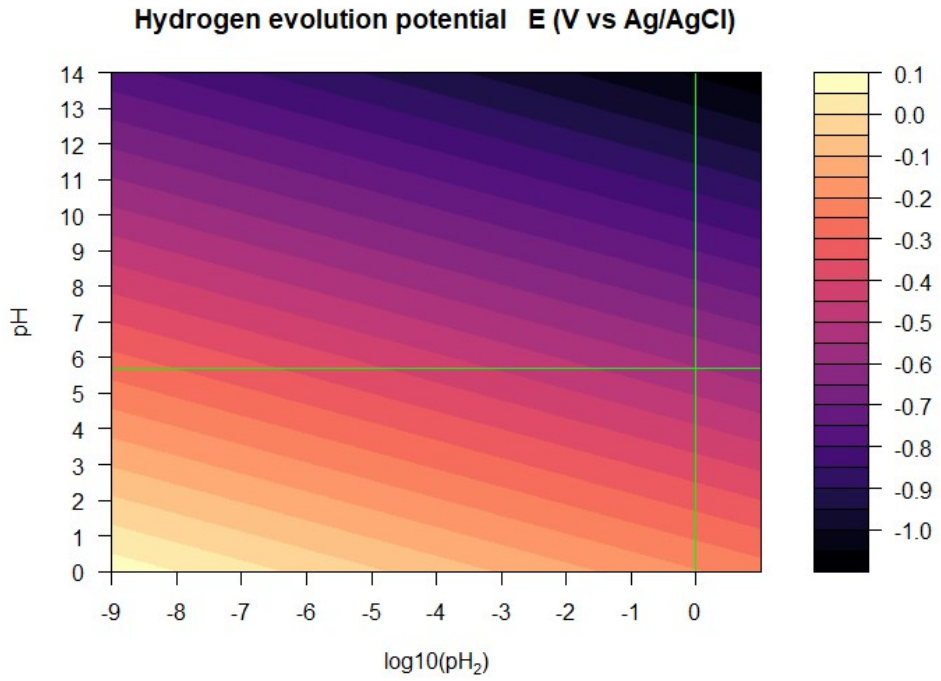

Figure S3. 2D contour plot showing the results of the modelling of the HER potential (indicated as V vs $Ag/AgCl_{sat\ KCl}$) based on the Nernst equation. The intersection between the two green lines indicates the cathode potential at which H_2 evolution starts at 37 °C with a pH of 5.7 and a H_2 partial pressure of 1: -548 mV.

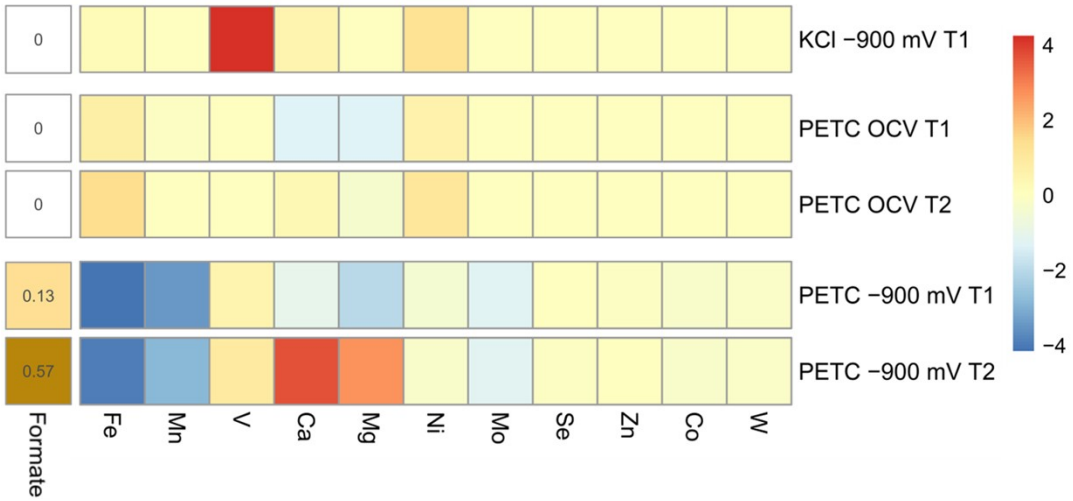

Figure S4. Heatmap indicating the concentration difference over time (in mg/L) relative to the starting point (T0: time zero) of the elements of interest in solution, analyzed by ICP-MS, in the electrolytes KCl: with an applied potential of -900 mV, PETC: without applied potential: OCV and PETC: with an applied potential of -900 mV. Formate concentrations (g/L), measured by HPLC, are also included. T1 indicates 1 week. T2 indicates 2 weeks. Average concentration difference is represented (n=3). KCl results are included as negative control for CO2RR to formate (n=2).

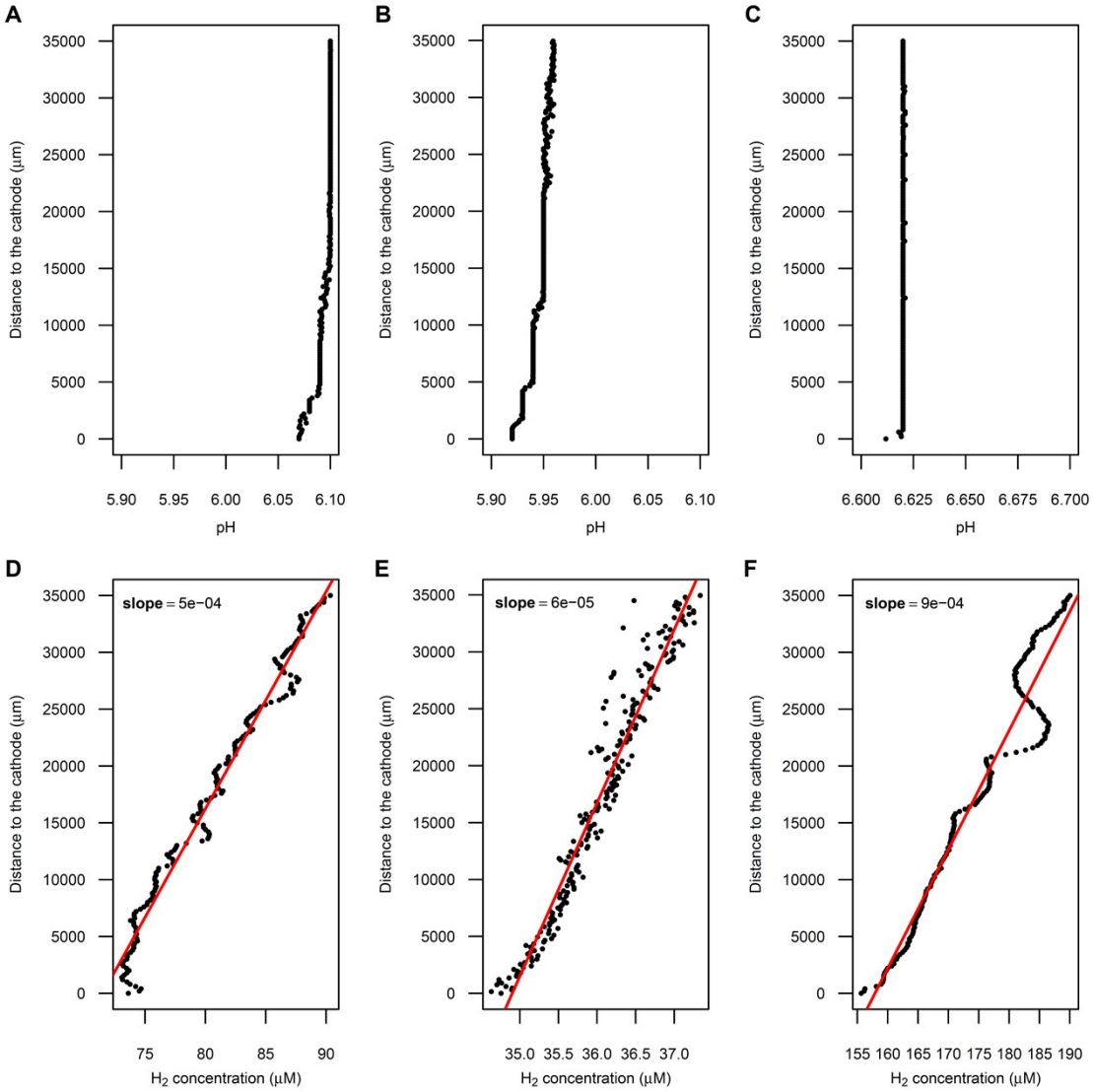

Figure S5. H_2 and pH *in-situ* profiles. pH gradients in abiotic **(a)**, biofilm-dominant **(b),** and planktonic-dominant **(c)** conditions measured from the cathode surface to 35 mm distance from the surface. H_2 gradients in abiotic **(d)**, biofilm-dominant **(e)** and planktonic-dominant **(f)** conditions measured from the cathode surface to 35 mm distance from the surface. Trend lines for dissolved H_2 profiles are marked in red, and the corresponding inversed slopes are presented inside the plots (µM/µm).

2.1 Discussion H_2 and pH *in-situ* profiles

To grow *C. ljungdahlii* in defined phenotypes depending on external factors, in this case the inoculation density, allowed us to evaluate the physicochemical conditions during both, planktonic-dominant and biofilm-dominant electrosynthesis. Dissolved H_2 and pH microprofiles were measured 15 days after inoculation (time of maximum acetate

production). The pH microprofiles, determined without stirring, showed almost no change over the liquid column (Figure S5A, B, C). However, the pH of the planktonic-dominated reactor was 0.7 pH units higher than in the biofilm reactor. The dissolved H_2 concentrations (Figure S5D, E, F) instead formed a gradient, with increasing concentration with increasing distance from the electrode surface, whereby modelled linear gradients were similar for the planktonic-dominant (slope = $5 \cdot 10^{-4}$ µM/µm) and abiotic (slope = $9 \cdot 10^{-4}$ µM/µm) measurements. However, in the biofilm-dominant measurement, the gradient was much lower indicating less hydrogen diffusion into the bulk solution (slope = $6 \cdot 10^{-5}$ µM/µm). H_2 concentrations at the electrode surface were also only half as high for the biofilm-dominant (35 µM at distance 0 µm) compared to the abiotic system (75 µM at distance 0 µm). This could reflect a stronger local sink for hydrogen in the proximity of the cathode, most likely the biofilm, or a detrimental effect of the biofilm for the H_2 formation. In the planktonic-dominant system the H_2 concentrations at the electrode surface were twice as high as for the abiotic operation (155 µM at distance: 0 µm) indicating HER promotion, e.g., by the cells or extracellularly released enzymes i.e., hydrogenases[4]. This difference in H_2 detection (or production) between planktonic-dominant and biofilm-dominant was observed in all performed experiments.

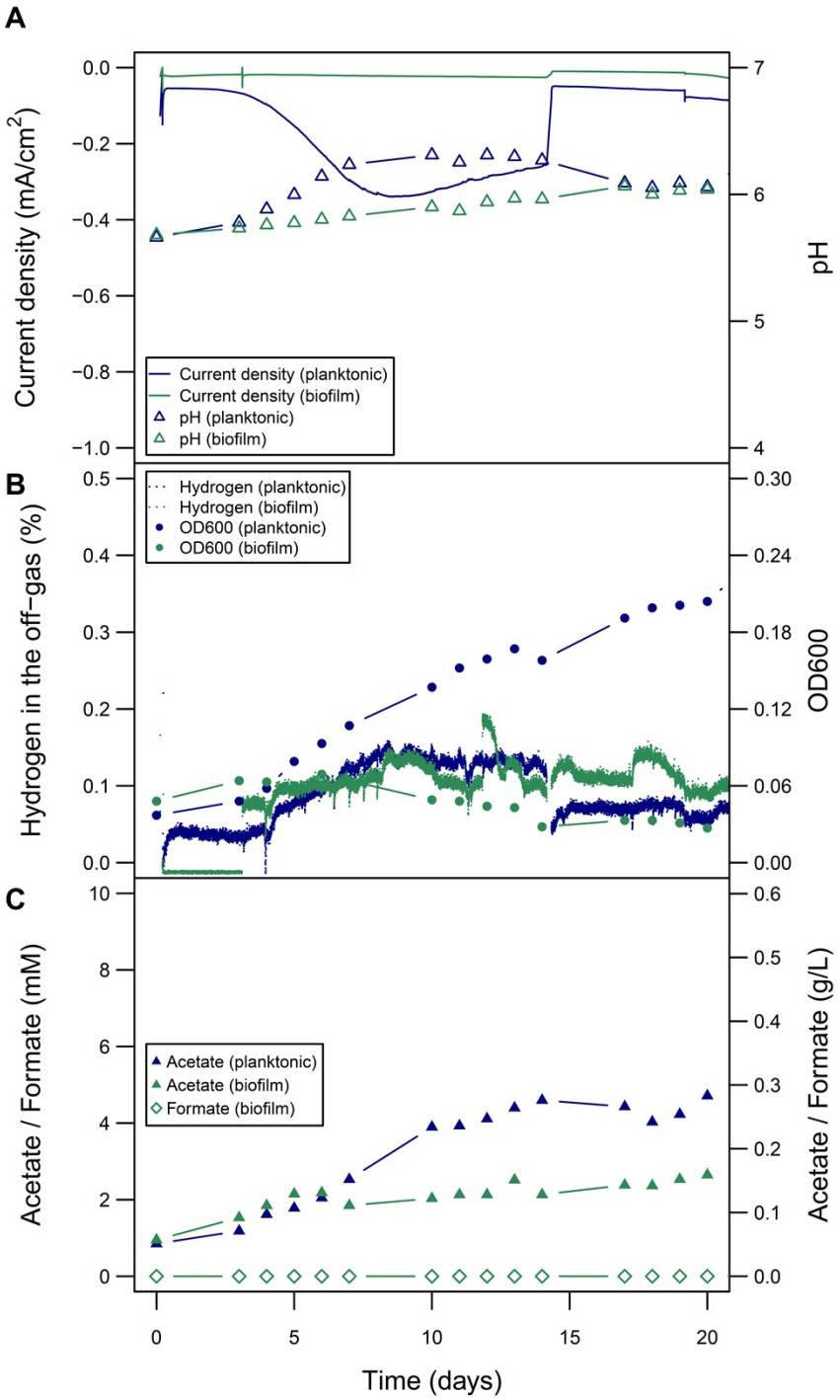

Figure S6. Independent replicate 1 of microbial electrosynthesis at fixed potential (-900 mV). Two reactors were inoculated with low cell density (biofilm-dominant, green traces) and high cell density (planktonic-dominant, blue traces) cultures, respectively. **(a)** Current density and pH development. **(b)** H_2 detected in the off-gas and OD600. **(c)** Acetate titers. Electrode surface area was 26.59 cm^2 with a surface-area-to-reactor-volume ratio of 66.48 cm^2/L.

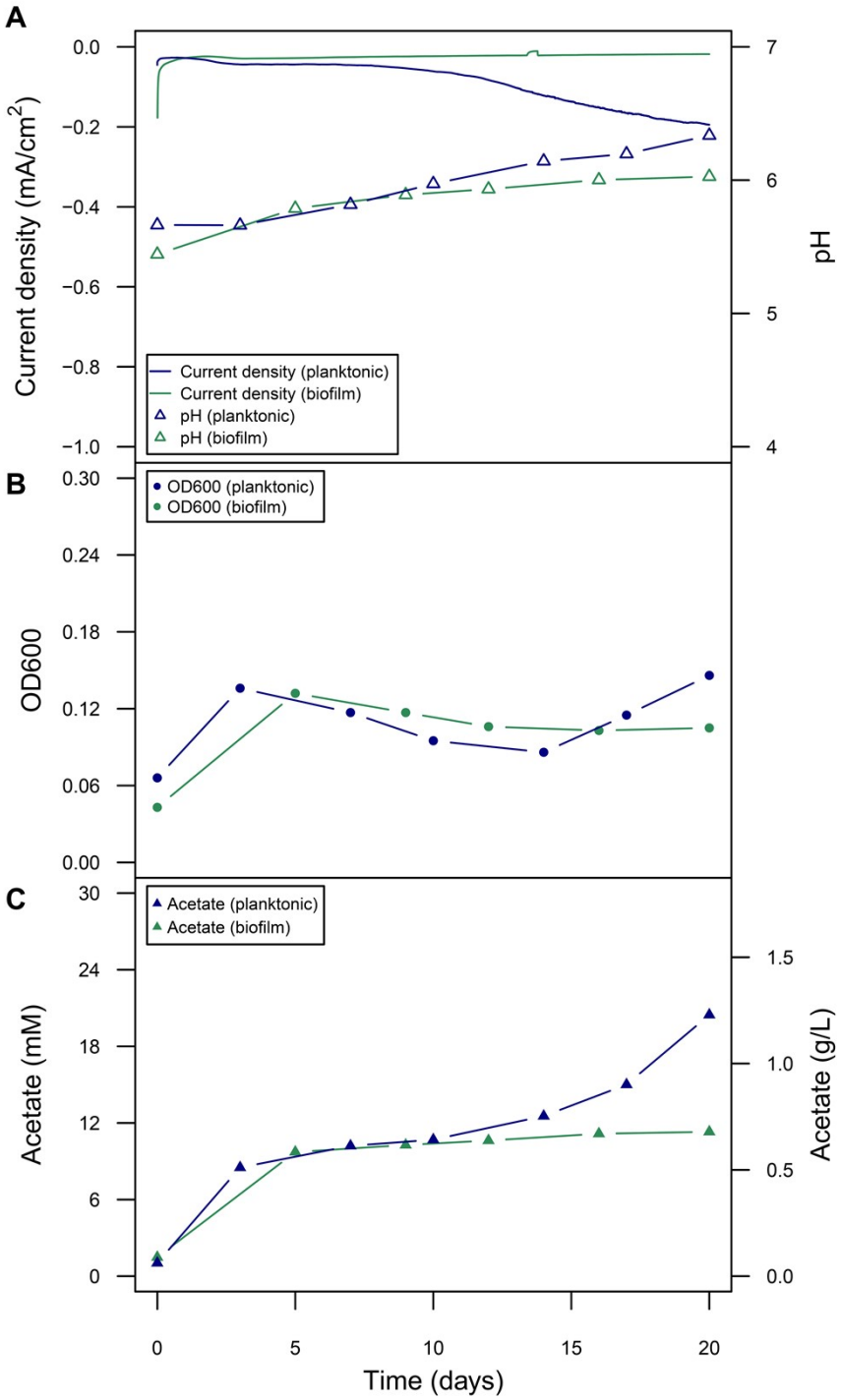

Figure S7. Independent replicate 2 of microbial electrosynthesis at fixed potential (-900 mV). Two reactors were inoculated with low cell density (biofilm-dominant, green traces) and high cell density (planktonic-dominant, blue traces) cultures, respectively. **(a)** Current density and pH development. **(b)** OD600. **(c)** Acetate titers. Electrode surface area was 26.59 cm^2 with a surface-area-to-reactor-volume ratio of 66.48 cm^2/L.

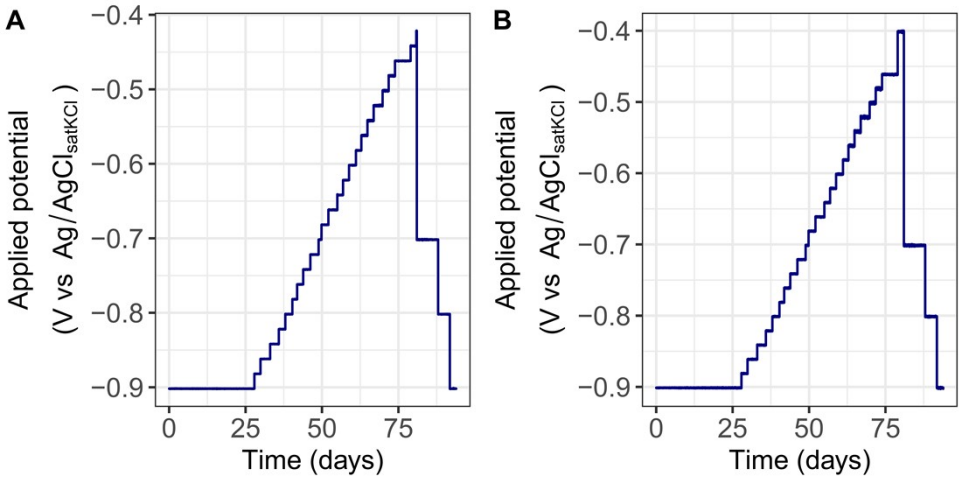

Figure S8. Stepwise gradients of increasing potentials corresponding to the data presented in Figure 5. **(a)** Reactor inoculated with low cell density (biofilm-dominant). **(b)** Reactor inoculated with high cell density (planktonic-dominant).

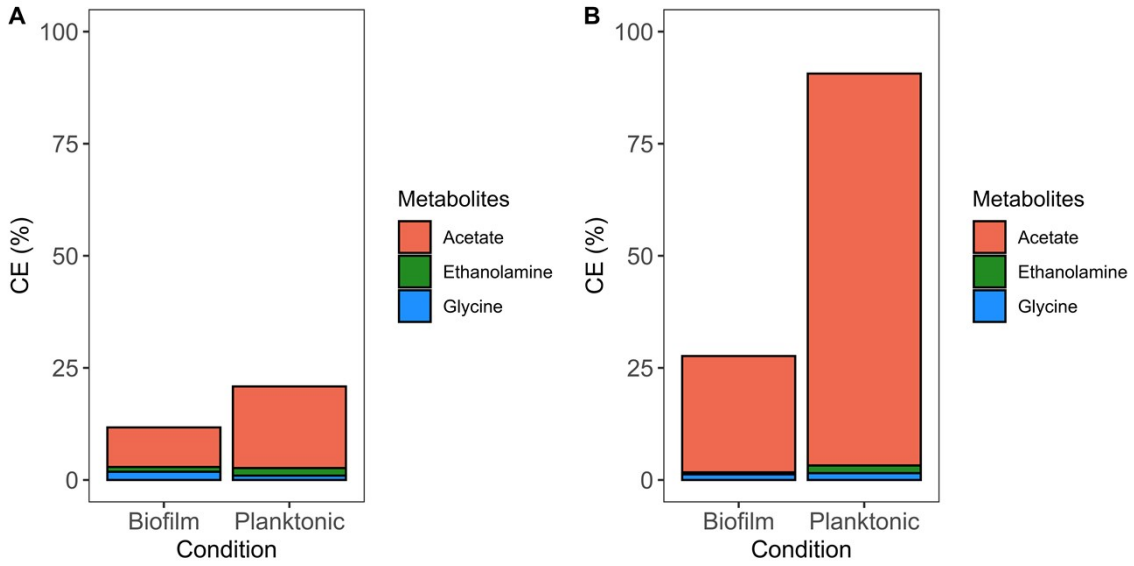

Figure S9. Stacked bar chart with the coulombic efficiencies (CE) grouped by metabolites. H_2 in the off-gas and biomass likely made up most of the gap to 100%. However, H_2 could not be included in this balance since the off-gas H_2 sensors only provide a relative composition. Biomass was estimated from cell count approximations. Biomass CE values were all below 1.5%, so they were not included in the chart. **(a)** MES with increasing potentials (data represented in Figure 5). Results calculated from day 10 to day 40. **(b)** MES with bigger electrodes (data represented in Figure 8). Results calculated from day 10 to day 40.

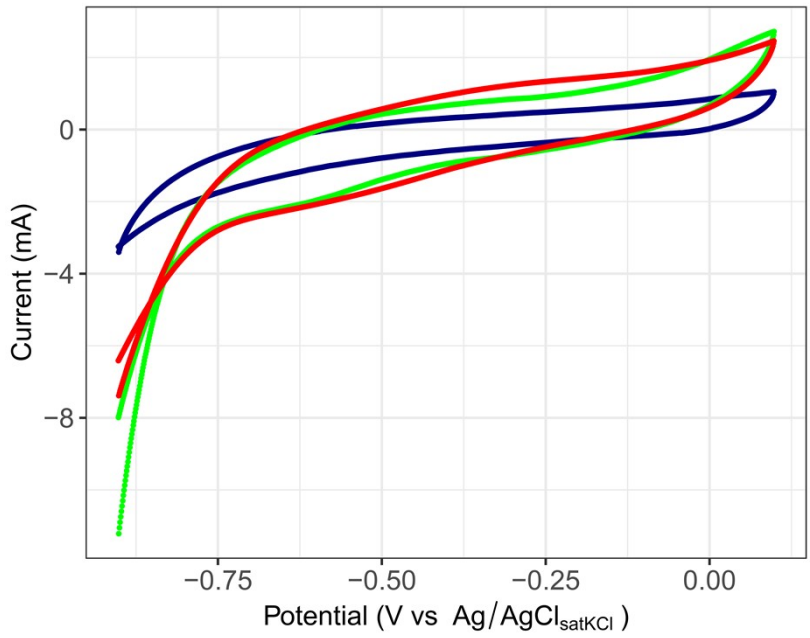

Figure S10. Cyclic voltammetry taken at different stages of a representative planktonic-dominant MES run: before inoculation (blue), early bacterial growth (green) and late bacterial growth (red). Scan rate: 1 mV/s. Scan number: 4.

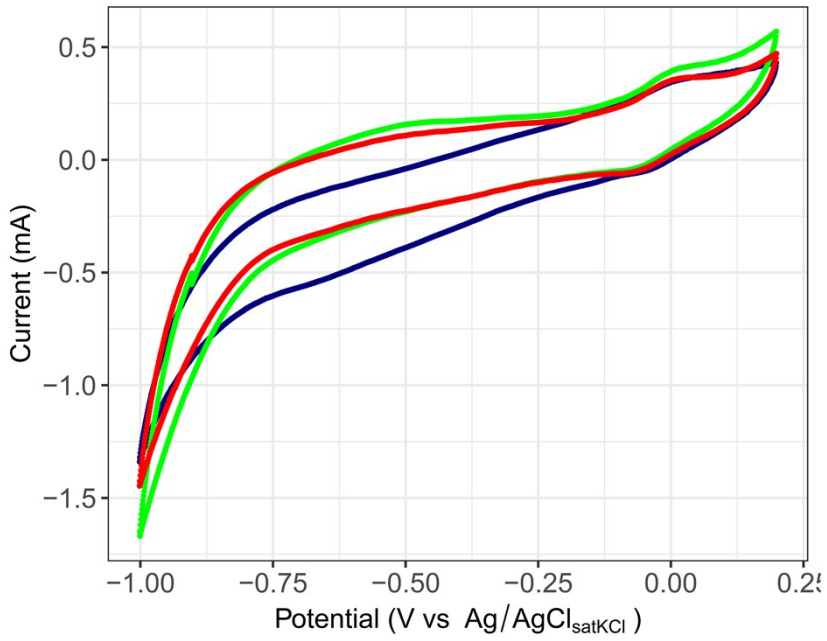

Figure S11. Cyclic voltammetry taken at different stages of a representative biofilm-dominant MES run: before inoculation (blue), early bacterial growth (green) and late bacterial growth (red). Scan rate: 1 mV/s. Scan number: 4.

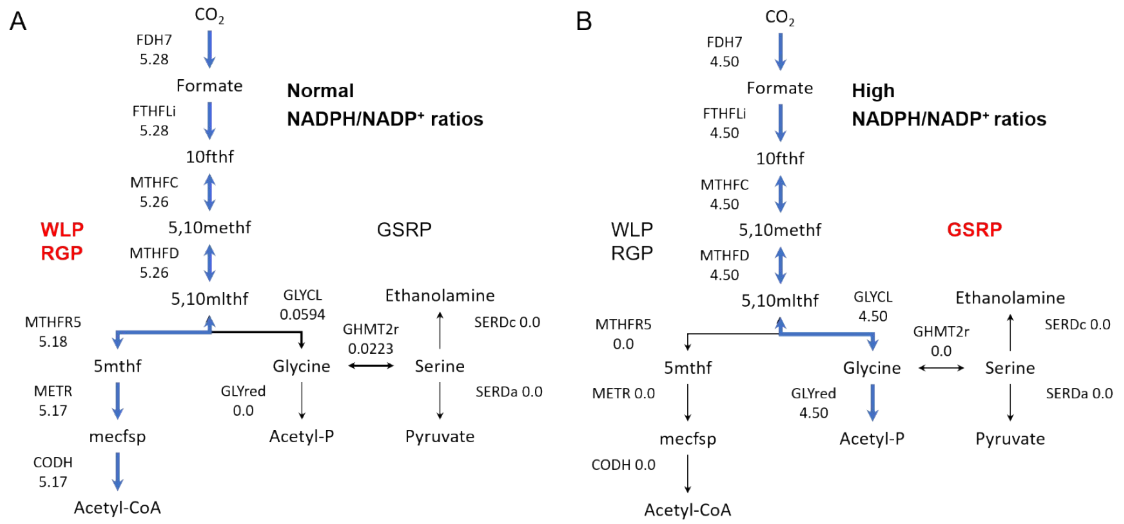

Figure S12. Schematic representation of the putative pathways for carbon fixation in *C. ljungdahlii*. The Wood-Ljungdahl pathway (WLP) is shown on the left side of each scheme, from CO_2 to acetyl-CoA. The reductive glycine pathway (RGP) is shown on the right side of each scheme, from CO_2 to serine. The glycine synthase-reductase pathway (GSRP) is shown on the right side if each scheme, from CO_2 to acetyl phosphate (acetyl-P). Flux values (mmol/gDW/h) are represented closed to the respective reaction name. Model reaction names: formate dehydrogenase – ferredoxin dependent (FDH7); formate-tetrahydrofolate ligase (FTHFLi); methenyltetrahydrofolate cyclohydrolase (MTHFC); methylenetetrahydrofolate dehydrogenase (MTHFD); 5,10-methylenetetrahydrofolate reductase (MTHFR5); methyltetrahydrofolate:corrinoid/iron-sulfur protein methyltransferase (METR); carbon monoxide dehydrogenase – acetyl-CoA synthase (CODH); glycine cleavage system (GLYCL); glycine reductase (GLYred); glycine hydroxymethyltransferase (GHMT2r); serine decarboxylase (SERDc); serine deaminase (SERDa). Metabolite names: 10-formyltetrahydrofolate (10fthf); 5,10-methenyltetrahydrofolate (5,10methf); 5,10-methylenetetrahydrofolate (5,10mlthf); 5-methyltetrahydrofolate (5mthf); methylcorrinoid iron sulfur protein (mecfsp).

2.2 Discussion genome-scale metabolic modelling

Using the iHN367[5] model of *C. ljungdahlii*, we made the glycine cleavage system reversible (GLYCL), the formate dehydrogenase irreversible (FDH7) and we adjusted the constraints of the hydrogenases; according to previous experiments[6] and our own data. We have chosen autotrophic medium (in accordance with the PETC recipe) in which the sole carbon and energy sources are CO_2 and H_2, respectively. Glycine reductase reaction (GLYred) was added to the model, and reversibility was corrected for the acetaldehyde: ferredoxin oxidoreductase (ACAFDOR), according to our own data and studies[7,8].

Code in Python to generate the model with Cobrapy:

```
# The objective is biomass: initial part of the growth
(acidogenesis)
import cobra
model = cobra.io.read_sbml_model("iHN637.xml")
# Change in reactions
model.reactions.get_by_id("GLYCL").lower_bound = -1000.0
model.reactions.get_by_id("FDH7").lower_bound = 0.0
model.reactions.get_by_id("HYDFDi").lower_bound = 0.0
model.reactions.get_by_id("HYDFDi").upper_bound = 0.0
model.reactions.get_by_id("HYDFDN2r").lower_bound = -10.0
model.reactions.get_by_id("HYDFDN2r").upper_bound = 10.0
model.reactions.get_by_id("HYDFDN").lower_bound = -1.0
model.reactions.get_by_id("HYDFDN").upper_bound = 1.0
model.reactions.get_by_id("ACAFDOR").lower_bound = -1000.0
model.reactions.get_by_id("ACAFDOR").upper_bound = 1000.0
# Change medium
medium = model.medium
medium["EX_fru_e"] = 0.0
medium["EX_co2_e"] = 20.0
medium["EX_h2_e"] = 80.0
medium["EX_for_e"] = 0.0
medium["EX_cys__L_e"] = 0.0
medium["EX_co_e"] = 0.0
model.medium = medium
# Removal of repeated reactions
model.reactions.GCCa.knock_out()
model.reactions.GCCb.knock_out()
model.reactions.GCCc.knock_out()
model.reactions.ACONTa.knock_out()
model.reactions.ACONTb.knock_out()
model.reactions.PFL.knock_out()
model.reactions.HYD2.knock_out()
# Addition Glycine reductase
reaction = cobra.Reaction("GLYred")
reaction.name = "Glycine/betaine reductase"
reaction.lower_bound = 0.0
reaction.upper_bound = 1000.0
reaction.add_metabolites({
    model.metabolites.gly_c: -1.0,
    model.metabolites.pi_c: -1.0,
    model.metabolites.h_c: -1.0,
    model.metabolites.nadph_c: -1.0,
    model.metabolites.nadp_c: 1.0,
    model.metabolites.actp_c: 1.0,
    model.metabolites.h2o_c: 1.0,
    model.metabolites.nh4_c: 1.0
})
reaction.gene_reaction_rule = "( CLJU_RS13500 or CLJU_RS13455 or
CLJU_RS13460)"
```

```
reaction.reaction
model.add_reactions([reaction])
```

The generated model was imported into Escher to proceed with the interactive flux balance analysis, which allowed the generation of Figure S10. Flux values for the normal NADPH/$NADP^+$ ratios were obtained maximizing the biomass reaction. Flux values for the high NADPH/$NADP^+$ ratios were obtained maximizing the Ferredoxin NADPH linked hydrogenase (HYDFDN2r) reaction.

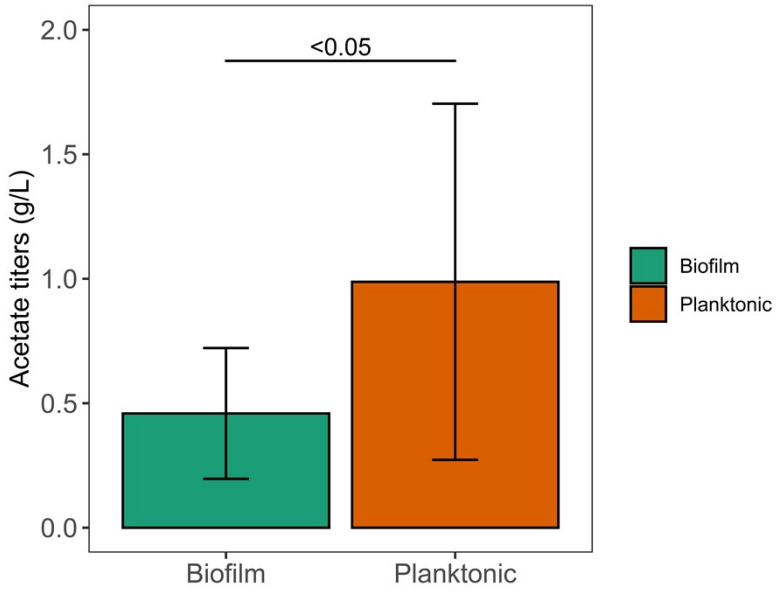

Figure S13. Bar chart comparing acetate titers after 20 days of electroautotrophic growth (in which biofilm-dominant or planktonic-dominant conditions were induced). Friedman rank sum test on a statistical design with blocks (to reduce the variance due to the use of different inocula) was performed, and significant differences ($p < 0.05$) were found between growth phenotypes.

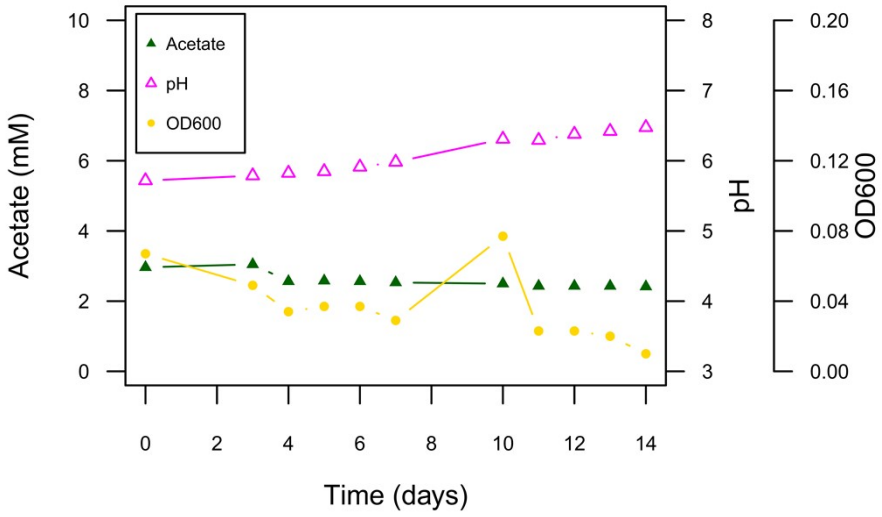

Figure S14. Negative control of microbial electrosynthesis with *C. ljungdahlii* at open circuit voltage (OCV). The reactor was inoculated with high cell density. Acetate titers, pH development and OD600 are shown. Electrode surface area was 26.59 cm^2 with a surface-area-to-reactor-volume ratio of 66.48 cm^2/L.

3. Additional table

Table S2. Gradient table of the HPLC method for the analysis of amino compounds.

(min)	A (%)	B (%)
1	90	10
10	80	20
20	60	40
25	40	60
27	40	60
28	90	10
39	90	10

4. Additional references

1 H. E. Streett, K. M. Kalis and E. T. Papoutsakis, *Appl. Environ. Microbiol.*, 2019, **85**, 1–15.

2 J. T. Heap, O. J. Pennington, S. T. Cartman and N. P. Minton, *J. Microbiol. Methods*, 2009, **78**, 79–85.

3 B. Molitor, K. Kirchner, A. W. Henrich, S. Schmitz and M. A. Rosenbaum, *Sci. Rep.*, , DOI:10.1038/srep31518.

4 J. S. Deutzmann, M. Sahin and A. M. Spormann, *MBio*, 2015, **6**, 1–8.

5 H. Nagarajan, M. Sahin, J. Nogales, H. Latif, D. R. Lovley, A. Ebrahim and K. Zengler, *Microb. Cell Fact.*, 2013, **12**, 118.

6 H. Richter, B. Molitor, H. Wei, W. Chen, L. Aristilde and L. T. Angenent, *Energy Environ. Sci.*, 2016, **9**, 2392–2399.

7 Y. Song, J. S. Lee, J. Shin, G. M. Lee, S. Jin, S. Kang, J. K. Lee, D. R. Kim, E. Y. Lee, S. C. Kim, S. Cho, D. Kim and B. K. Cho, *Proc. Natl. Acad. Sci. U. S. A.*, 2020, **117**, 7516–7523.

8 J. Lo, J. R. Humphreys, J. Jack, C. Urban, L. Magnusson, W. Xiong, Y. Gu, Z. J. Ren and P. C. Maness, *Front. Bioeng. Biotechnol.*, 2020, **8**, 1247.